

Available online at [www.sciencedirect.com](http://www.sciencedirect.com)

Biochimica et Biophysica Acta 1768 (2007) 598–608

[www.elsevier.com/locate/bbamem](http://www.elsevier.com/locate/bbamem)

## Structural correlates of antimicrobial efficacy in IL-8 and related human kinocidins

Nannette Y. Yount<sup>a,b</sup>, Alan J. Waring<sup>a,c</sup>, Kimberly D. Gank<sup>a,b</sup>, William H. Welch<sup>d</sup>,  
Deborah Kupferwasser<sup>a,b</sup>, Michael R. Yeaman<sup>a,b,c,\*</sup>

<sup>a</sup> Division of Infectious Diseases, LAC-Harbor UCLA Medical Center, Torrance, CA 90509, USA

<sup>b</sup> St. John's Cardiovascular Research Center, Torrance, CA 90502, USA

<sup>c</sup> Department of Medicine, David Geffen School of Medicine at UCLA, Los Angeles, CA 90024, USA

<sup>d</sup> Department of Biochemistry, University of Nevada, Reno, NV 89557, USA

Received 9 August 2006; received in revised form 18 October 2006; accepted 13 November 2006

Available online 30 November 2006

### Abstract

Chemokines are small (8–12 kDa) effector proteins that potentiate leukocyte chemo-navigation. Beyond this role, certain chemokines have direct antimicrobial activity against human pathogenic organisms; such molecules are termed kinocidins. The current investigation was designed to explore the structure–activity basis for direct microbicidal activity of kinocidins. Amino acid sequence and 3-dimensional analyses demonstrated these molecules to contain iterations of the conserved  $\gamma$ -core motif found in broad classes of classical antimicrobial peptides. Representative CXC, CC and C cysteine-motif-group kinocidins were tested for antimicrobial activity versus human pathogenic bacteria and fungi. Results demonstrate that these molecules exert direct antimicrobial activity *in vitro*, including antibacterial activity of native IL-8 and MCP-1, and microbicidal activity of native IL-8. To define molecular determinants governing its antimicrobial activities, the IL-8  $\gamma$ -core (IL-8 $\gamma$ ) and  $\alpha$ -helical (IL-8 $\alpha$ ) motifs were compared to native IL-8 for antimicrobial efficacy *in vitro*. Microbicidal activity recapitulating that of native IL-8 localized to the autonomous IL-8 $\alpha$  motif *in vitro*, and demonstrated durable microbicidal activity in human blood and blood matrices *ex vivo*. These results offer new insights into the modular architecture, context-related deployment and function, and evolution of host defense molecules containing  $\gamma$ -core motifs and microbicidal helices associated with antimicrobial activity.

© 2006 Elsevier B.V. All rights reserved.

**Keywords:** Antimicrobial; Peptide; Structure; Chemokine

### 1. Introduction

Chemokines comprise a class of small secretory cytokines that play important roles in potentiating leukocyte chemo-navigation and host defense activity. More than 40 human chemokines have been characterized and are classified into four groups according to conserved N-terminal cysteine motifs: CXC ( $\alpha$ -chemokines), CC ( $\beta$ -chemokines), C, and CX<sub>3</sub>C. Chemokines have been identified in vertebrates as distant as teleost fish, and are expressed in a broad array of mammalian cell types including myeloid, endothelial, epithelial and fibroblast lineages [1]. Of the chemokines, interleukin-8 (IL-8; or CXC-ligand 8 [CXCL8]) is perhaps the best characterized, having been first identified as neutrophil-activating factor from human monocytes more than 15 years ago [2,3].

**Abbreviations:** PF-4, platelet factor 4; PMP, platelet microbicidal protein; PBP, platelet basic protein; CTAP-3, connective tissue-activating peptide 3;  $\beta$ -TG, beta thromboglobulin; NAP-2, neutrophil activating peptide-2; RANTES, releasable upon activation, normal T cell expressed and secreted; CXC, cysteine-X-cysteine; CC, cysteine-cysteine; CXCR, CXC receptor; CCR, CC receptor; YNB, yeast nitrogen broth; QSAR, quantitative structure–activity relationship; CD, circular dichroism; F-moc, (9-fluorenyl-methyloxycarbonyl); TFA, trifluoroacetic acid; MALDI-TOF, matrix-assisted laser desorption ionization time-of-flight; PIPES, piperazine-*N,N'*-bis[2-ethanesulfonic acid]; Da, daltons, and standard single letter codes for amino acids

\* Corresponding author. David Geffen School of Medicine at UCLA, Division of Infectious Diseases, Harbor-UCLA Medical Center, 1124 West Carson Street, RB-2, Torrance, CA 90502, USA. Tel.: +1 310 222 6428; fax: +1 310 782 2016.

E-mail address: [MRYeaman@ucla.edu](mailto:MRYeaman@ucla.edu) (M.R. Yeaman).

Several teleologic parallels exist between chemokines and classical antimicrobial peptides. Like chemokines, antimicrobial peptides are typically small, amphipathic, and cationic effectors of innate immunity, and are found in organisms across the phylogenetic spectrum [4]. Moreover, many chemokines and antimicrobial peptides are expressed at low levels in unstimulated host cells, but are rapidly upregulated 10- to 100-fold upon exposure to relevant stimuli, including microbial components [1]. The fact that certain antimicrobial peptides are chemotactic reinforces further functional reciprocity between antimicrobial peptides and chemokines [5]. Duality in microbicidal and chemokine functions of such host defense peptides suggests important biological links between classical antimicrobial peptides and microbicidal chemokines, as well as molecular and cellular innate immune responses.

While chemokines have not traditionally been ascribed with direct antimicrobial activities, evidence for such functions is mounting. Direct antimicrobial efficacy has been demonstrated for the platelet chemokines PF-4, platelet basic peptide (PBP) and its derivative CTAP-3 [6–8], and truncations thereof [9]. Direct antimicrobial activity has also recently been confirmed for other chemokines [10,11]. Hence, the term kinocidin (*kino*—chemokine; *cidin*—microbicidal) has been applied to encompass chemokines with direct microbicidal activity [4,8,12]. Despite immunological likeness to other kinocidins, the direct antimicrobial activity of well-characterized chemokines such as IL-8 has only recently been recognized [4,12–14]. For example, although Bjorstad et al. described antibacterial activity of an IL-8-derived peptide [14], their studies did not demonstrate antimicrobial activities of native (full-length) IL-8 *in vitro*, or microbicidal efficacy of these molecules in human blood or blood matrices. Thus, the present investigations were conducted to seek new insights into the antimicrobial structures and functions of human kinocidins, including IL-8.

The current studies provide important new information regarding complementary host defense roles of kinocidins. Primary sequence and 3-dimensional analyses revealed that kinocidins possess iterations of the hallmark  $\gamma$ -core signature present in broad classes of cysteine-stabilized antimicrobial peptides and other host defense effector proteins [4]. Moreover, current data demonstrate diverse kinocidins exert differential antimicrobial efficacies and spectra under pH conditions pertinent to infection and inflammation. These findings support our hypothesis that certain kinocidins are evolved to exert optimal host defense functions in specific contexts [4,12,13]. Synthetic congeners corresponding to  $\alpha$ -helical and  $\gamma$ -core domains of IL-8 distinguished the direct versus indirect antimicrobial functions of these respective modules. Moreover, these studies revealed a previously undetected direct fungicidal activity of the IL-8 helix versus *Candida albicans*. Collectively, these results demonstrate that human kinocidins contain iterations of  $\gamma$ -core motifs present in classical antimicrobial peptides, configured with  $\alpha$ -helical motifs that likely mediate their antimicrobial activity. These motifs are integrated in a modular form within kinocidins, facilitating autonomous dissociation of the helix to exert microbicidal efficacy in relevant contexts of blood matrices.

## 2. Materials and methods

### 2.1. Native molecules

Recombinant human chemokines (IL-8, RANTES, GRO- $\alpha$ , MCP-1, PF-4, and lymphotactin [Biosource International, Camarillo, CA]), and human neutrophil defensin-1 (HNP-1 [Peptides International, Louisville, KY]) were obtained commercially.

### 2.2. Peptide synthesis and authentication

IL-8 structural domains were generated by F-moc solid-phase synthesis:  $\gamma$ -core (ANTEIVKLSGRELCLDP; IL-8 $\gamma$ ), and  $\alpha$ -helix (KENWVQRV-VEKFLKRAENS; IL-8 $\alpha$ ). Peptides were purified by RP-HPLC as previously described ([15]; >95% purity), and authenticated by amino acid analysis (Molecular Structure Facility, University of California, Davis) and MALDI-TOF spectrometry (UCLA Spectrometry Facility). Experimentally determined masses were within standard confidence intervals ( $<\pm 0.1\%$  of calculated molecular weight).

### 2.3. Antimicrobial assays

Antimicrobial assays were performed against a panel of prototype human pathogens as previously detailed [4]: *Staphylococcus aureus* (ATCC 27217; Gram-positive bacterium); *Salmonella typhimurium* (5996s; Gram-negative bacterium); and the fungus *Candida albicans* (ATCC 36082). All assays were conducted a minimum of two independent times with multiple replicates. Results of independent assays were analyzed using Wilcoxon Rank Sum analysis with Bonferroni correction for multiple comparisons.

#### 2.3.1. Solid-phase assay

Mid-logarithmic phase organisms were prepared, introduced into buffered agarose (PIPES [10 mM, pH 7.5] or MES [2.0 mM, pH 5.5]) to achieve final inocula of  $10^6$  CFU/ml, and poured into plates. Peptides (0.5 nmol/well [50 nmol/ml]) were added to wells in the seeded matrix, and incubated for 3 h at 37 °C. Nutrient overlay medium was applied, and assays incubated at 37 °C or 30 °C for bacteria or fungi, respectively. After 24 h, zones of inhibition were measured, and results recorded as zones of complete or partial inhibition. Defensin HNP-1 was included in each assay as an internal control. Zones of inhibition were measured in millimeters as the radius of the cleared region minus the well diameter. This assay reflects microbiostatic (inhibition) and/or microbicidal (killing) activities, but does not distinguish these effects.

#### 2.3.2. Solution-phase assay

Organisms were prepared and adjusted to  $10^6$  CFU/ml in PIPES or MES buffer as above but lacking agarose, and dispensed ( $5 \times 10^4$  CFU per 50  $\mu$ l aliquot). Peptide (concentration range, 20–0.00125 nmol/ml) was introduced into the assay medium, and incubated for 1 h at 37 °C. After incubation, media were serially diluted and plated in triplicate for enumeration.

#### 2.3.3. Biomatrix assay

Antimicrobial activity of IL-8 $\alpha$  in human whole blood and homologous plasma and serum fractions was assessed in an *ex vivo* biomatrix assay developed to assess antimicrobial polypeptide efficacy in complex human blood matrices [16]. For biomatrix studies, the well-characterized *Escherichia coli* strain ML-35 was used as the target organism in this system [16]. This strain is resistant to serum, ideal for use in assessing peptide antimicrobial activity in blood and blood-derived matrices [16]. Organisms were cultured to mid-logarithmic phase in brain–heart infusion broth (Difco Laboratories, Detroit, Mich.) at 37 °C, washed, and resuspended in PBS (Irvine Scientific; pH 7.2). Inocula were quantified spectrophotometrically and validated by quantitative culture. Biomatrices (whole blood, plasma, or serum) were distributed in 85- $\mu$ l aliquots into 96-well microtiter plates (Corning Glass Works, Corning, N.Y.) Peptide (5  $\mu$ l; concentration range 1–50  $\mu$ g/ml) was added either simultaneously with the microorganism (final inoculum,  $10^5$  CFU/ml in a 10  $\mu$ l volume), or after a 120 min pre-incubation period in the biomatrix to assess durability of peptide

efficacy. Concurrent controls were performed using Mueller–Hinton broth (MHB) per guidelines of the Clinical Laboratory Standards Institute [17]. The mixtures were incubated with constant agitation for 2 h at 37 °C. After incubation, aliquots were diluted and quantitatively cultured in triplicate onto blood agar. Surviving organisms were enumerated as CFU/ml. Experiments were performed a minimum of two independent times on different days and with different blood donor sources.

## 2.4. Structure analyses

Complementary methods were used to analyze polypeptide structures in this investigation:

### 2.4.1. Bioinformatics

Protein structure data were obtained from the National Center for Biotechnology Information (NCBI), and visualized using Protein Explorer [18]. Multiple sequence alignments were performed using Clustal [19] and 3-dimensional structures were analyzed and visualized using Protein Explorer [18]. Structural alignments were carried out using combinatorial extension, as quantified by root mean square deviation (RMSD) analysis [20].

### 2.4.2. Spectrometry

Secondary structures of IL-8 peptide domains were assessed by circular dichroism (CD) as previously noted [21]. Spectra were recorded with an AVIV 62DS spectropolarimeter (Aviv Biomedical Inc.). In brief, the purified peptides were solubilized (50 µg/ml in 50 mM NH<sub>4</sub>HCO<sub>3</sub>; pH 5.5 or 7.5) and scanned using a 0.1-mm light path from 260 to 185 nm (rate, 10 nm/min; sample interval, 0.2 nm; 25 °C). A mean of 8 buffer-subtracted spectra were deconvoluted into helix, β-sheet, turn, and extended structures using Selcon [22] and Dichroweb [23]; [cryst.bbk.ac.uk/cdweb](http://cryst.bbk.ac.uk/cdweb)) as indicated [21,24,25].

### 2.4.3. Computational modeling

Three-dimensional models of IL-8 domains were created using complementary methods [8]. Homology [SWISSMODEL, BLAST2P; [26,27]], dynamic alignment (SIM) [28] and refined match (ProModII) algorithms were used to identify modeling templates. In a parallel strategy, IL-8 amino acid sequences were converted to putative solution conformations by threading methods (Matchmaker [29]; Gene-Fold [30]) implemented with SYBYL software (Tripos Associates, St. Louis, MO). Target conformers were refined using AMBER95 force field and molecular dynamics [31]. In alternative approaches, molecular dynamics were executed without 0.4 kJ constraint penalties for canonical Ramachandran φ and ψ angles.

## 3. Results

### 3.1. Iterations of the γ-core motif in human kinocidins

A bioinformatics approach was used to specify and compare phylogeny and structural homology in human kinocidins [4]. Sequence and 3-dimensional analyses of more than 30 human C, CC, and CXC kinocidins demonstrated iterations of antimicrobial peptide γ-core motifs [γ<sub>AP</sub>; [4,32]], and that the central β-sheet domain comprising this motif corresponds to the most highly conserved domains within mature kinocidins (Fig. 1). Congruent with the γ<sub>AP</sub> motif, the kinocidin γ-core [γ<sub>KC</sub> core; [32]] motif is comprised of a 13–17 residue anti-parallel β-hairpin, containing a central hydrophobic region that is typically

Sequence Formula	C (X <sub>10,11</sub> )	G (X <sub>2</sub> )	C (X <sub>3</sub> )	P		
GSEVSDKRTCVSLTTQRLPVSRIKTYTITE-GSL---	--RAVIFITK--RGLKVCADP				QATWVRDVVRSMDRKSNTRN	XCL1 LYM
ASVATELRCCQLTQLGHIHPKNIQSVNVKSP-GPH---	CAQTEVIATLK--NGRKA				CNPASPIVKKIIEKMLNSDKS	CXCL1 GRO-α
LATELRCCQLTQLGHIHLKNIQSVNVKSP-GPH---	CAQTEVIATLK--NGKAC				CNPASPMVKKIIIEKMLKNGKSN	CXCL2 GRO-β
EAEEDGDLQCLCVKTTTSQVRPHITSLEVIKA-GPH---	CPTAQLIATLK--NGRKI				CLDLQAPLYKKIIEKMLLES	CXCL4 PF-4
AVLRELRCCVCLQTTQGVHPKMI SNLQVFAI-GPQ---	CSKVEVVASLK--NGKEI				CLDPEAPFLKVKVIQKILDGGNKEN	CXCL5 ENA-78
AVLTELRCCLRVTLRVNPKTI GKLQVFPFA-GPQ---	CSKVEVVASLK--NGKQC				CLDPEAPFLKVKVIQKILDSGNKSN	CXCL6 GCP-2
DLYAELRCMCIKTTSGHIHPKNIQSVLEVIGK-GTH---	CNQVEVIATLK--DGRKI				CLDLDAPRIKKIVQKLAGDESAD	CXCL7 PBP
SAKELRCQCICKTYSKPFHPKFIKELRVIESGPH---	CANTEIIV--KLSD				GRELDPKENVWQVRVVEKFLKRAENS	CXCL8 IL-8
GRCSICISTNQGTHLQSLKDLKQFAPSPS---	CEKIEIATLK--NGVQT				CLNPDSDADVKELIKKWEKQVSKKKQK *	CXCL9 MIG
VRCTCISISNQPVNPRSLKLEIIPASQF---	CPRVEIATMK--KKGKR				CLNPESKAIKNLLKAVSKERSKRS	CXCL10 IP-10
GRCLIGPGVKAVKVADIEKASIMYPSNN---	CDKIEVIITLKENKG				QRCLNPKSKQARLIIEKVERKNF	CXCL11 I-TAC
YRCPCCRFESHVARANVHKHLKILNTPN---	CALQ-IVARLK--NNNR				QVGDIDPKLKWIQEYLEKALNKRFKM	CXCL12 SDF-1
LRCRCVQESSVFIPRRFIDRIQILPRGNG---	CPRK-EIIVVK--KNKSI				VDPQAEWIQRMMELVRKRSSTLPVP *	CXCL13 BCA-1
FSRC-CFSFAEQEIPRALICYRNT--SSI---	CNEGLIFLKL--RGKEA				CALDVTGWWQRHRKMLRHCPSKRK	CCL1 I-309
PITC-CFNVINRKIPQRLESYTRIT-NIQ---	CPKEAVIFKTK--RGKEV				CADPKERWVRDSMKHLDQIFQNLKP	CCL8 MCP-2
PSTC-CFTFSSKKISLQRLKSYVIT--SR---	CPQKAVIFRTK--LGKEI				CADPKKQVQNMKMLGRKAHTLKT	CCL13 MCP-4
SEC-CFTYTYKIPQRIMDYETN--SQ---	CSKPGVIFITK--RGKIV				GTNPSSDKWVQDYIKDKMKN	CCL14 HCC-1
FHFAADC-CTSYSISQSIPLMSKSYFET--SSE---	CSKPGVIFLTK--KGRQV				CAKPSGPGVQDCMKKLPYSI	CCL15 HCC-2
REC-CLEYFKGAIPLRKLKTWYQT--SED---	CSRDAIVFVT--QGRAI				CSDPNNKRVRKNAVKYQLSLERS	CCL17 TARC
ELC-CLVYTSWQIPKFIVDYSET--SPQ---	CPKPGVILLTK--RGRQI				CADPNKKWVQDYISDLKNA	CCL18 PARC
EDC-CLSVTQKPIPGYIVRNPHYLLIKDG---	GRVPAVVFTTL--RGRQL				CAPPDQPWVERIQRQLQRTSAKMKRRS	CCL19 MIP-3β
FHATSADC-CISYTPRSIPCSLLESYFETN--SE---	CSKPGVIFLTK--KGRRF				CANPSSDKQVQVCVRMLKLDTRIKTRKN	CCL23 MIPF-1
SPC-CMFFVSKRIPENRVVSYQLSSR--ST---	CLKAGVIFTTK--KQQFC				GDPKQEWVQRYMKNLDAKQKASPRAS *	CCL24 MIPF-2
QPDAINAPVTC-CYNFTNRKISVQRLSAYRRIT--SSK---	CPKEAVIFKTI--VAKEI				CADPKQKVVQDSMDHLDKQTQTPKT	CCL2 MCP-1
TAC-CFSYTSRQIPQNFADYFET--SSQ---	CSKPGVIFLTK--RSRQV				CADPSEEWVQKYVSDLELSA	CCL3 MIP-1α
TAC-CFSYTARKLPRNFVVDYET--SSL---	CSQPAVVFQTK--RSKQV				CADPSESWVQYVYDLELN	CCL4 MIP-1β
SPYSSDTPC-CFAYIARPLRAHIEKFYYS-G-K---	CSPAVVFVTR--KNRQV				CANPEKKWVREYINLSMS	CCL5 RANTES
STTC-CYRFINKKIPQRLESYRRIT--SSH---	CPREAVIFKTK--LDKEI				CADPTQKVVQDFMKHLDKKTQTPKL	CCL7 MCP-3
PTTC-CFNLANKRIPQRLESYRRIT--SGK---	CPKAVIFKTK--LAKDI				CADPKKKVVQDSMKYLDQKSPTPKP	CCL11 MCP-2
STC-CLKYYEKVLPRLRVVGYRKALN-----	CHLPAIFVTK--NRREI				GTNPNDWVQYIKDPLNPLLPTRNLS *	CCL16 HCC-4
FDC-CLGYTDRI LHPKFI VGFTRQLANEG---	CDINAIFHTK--KLSV				CANPKQTVVYIVRLLSKKVKNM	CCL20 LARC
QDC-CLKYSQRKIPAKVRSYKQEPSLG---	CSPAILFLPRKRSQAL				CADPKELVWQQLMQHLDKTPSPQKPAQ *	CCL21 SLC
SVC-CRDYVRYRLPLRVVGHFYWTS--DS---	CPRPGVLLTF--RDKEI				CADPRVPVWKMILNKLQ	CCL22 MDC
FEDC-CLAYHYPIGWA VLRRAWTYRIQEVSGS-	CNLPAAIFYLP--KRHRK				VGNPKSREVQRAMKLLDARNKVFALH *	CCL25 TECK
TAC-CTQLYRKPLSKLLRKKVIQVLEQADGD	CHLQAFVLH--LAQRS				CIHPQNPSSLQWFEHQERKLGHTLPKL *	CCL27 CTACK
SSC-CTEVSHHISRLLERLVNMCRIQRADGD-	CDLAAVILHV--KRRRI				CVSPHNHTVVKQWMMVQAAKKNKGKGNVC *	CCL28 MEC

γ<sub>KC</sub> core Signature

Fig. 1. Alignment of C, CC and CXC class human chemokines. The highlighted GX<sub>3</sub>C motif [glycine (G), orange; cysteine (C), yellow; proline (P), aqua] corresponds to the γ<sub>KC</sub> core signature (outlined in red). Conserved cysteine residues beyond the γ<sub>KC</sub> core are shaded gray. Gaps were introduced to achieve maximal alignment; \* Indicates truncated sequence.

Table 1  
Comparative physicochemical properties of human kinocidins and  $\alpha$ -helical domains thereof

Class	Classification schema		Native molecule				$\alpha$ -Helical domain				
	Ligand ID	Name	AA	M	Q	pI	AA $_{\alpha}$	Q $_{\alpha}$	M $_{\alpha}$	pI $_{\alpha}$	H $_{\alpha}$
CXC	CXCL8	IL-8	71	8299	+4	9.0	17	+2	2103	10.0	6.70
CXC	CXCL4	PF-4	70	7769	+3	8.8	13	+3	1573	9.8	6.12
CXC	CXCL1	GRO- $\alpha$	72	7751	+6	9.5	16	+2	1843	9.6	4.71
CC	CCL2	MCP-1	76	8685	+6	9.4	19	0	2287	6.8	5.35
CC	CCL5	RANTES	68	7851	+5	9.2	13	0	1655	6.1	6.71
C	CL1	Lymphotactin	92	10,173	+9	10.6	14	+2	1735	10.7	3.73

Physicochemical parameters are abbreviated for the native or  $\alpha$ -helical domain ( $\alpha$ ): AA, amino acids; M, average mass (in Daltons); Q, calculated charge at pH 7.0; pI, estimated isoelectric point [54]; H, hydrophobic moment [55].

flanked by basic residues. In kinocidins, the GXC consensus seen in the  $\gamma_{AP}$  core is modified such that a GX<sub>3</sub>C pattern is often observed within the central  $\beta$ -sheet domain. The following sequence formula can be used to describe the  $\gamma_{KC}$  motif found in the vast majority of all kinocidins:



Exceptions to this consensus formula can be noted in support of the rule. In some cases, there is variability at the G position, with the most common substitutions being a cationic (K, R) or amidated (Q, N) residue. This finding is consistent with concentration of positive charge propensity as has been identified in the  $\gamma$ -core motif of antimicrobial peptides [4]. In two instances (CXCL4 [PF-4], CCL1 [I-309]), the ultimate proline residue is absent, and in one case (XCL1 [LYM]) the initial cysteine is deleted. Nonetheless, all known kinocidins contain a  $\gamma$ -core sequence signature or iteration (Fig. 1).

Human IL-8 contains the sequence: NH<sub>2</sub>···CANTEIIVKLS-DGRELCLDP···COOH. This sequence is consistent with the consensus  $\gamma_{KC}$ -core motif. Furthermore, many kinocidins exhibit similar physicochemical properties (Table 1) and a recurring amino acid position pattern adhering to the consensus  $\gamma_{KC}$  core formula (Table 2).

### 3.2. Comparative antimicrobial activities of CXC, CC, and C group kinocidins

To compare their relative antimicrobial activities, prototypic members of the CXC, CC, and C-group kinocidins were evaluated versus a panel of prototypic pathogens in three distinct but complementary assays:

#### 3.2.1. Solid-phase assay

The antimicrobial activities of study kinocidins were compared in a sensitive and pH-specific radial diffusion assay [4] (Fig. 2). Each of the representative kinocidins studied had direct antimicrobial activity in one or more conditions tested in this assay system (Fig. 3). It is also significant to note the diversity of antimicrobial spectra and conditional optima for distinct kinocidins (Fig. 3). In many cases, kinocidins exerted pathogen- or pH-specific activities that differed from those of the classical antimicrobial peptide, HNP-1. Although study kinocidins had pI values  $\geq 8.5$  (Table 1), neither net charge nor pI directly correlated with antimicrobial activity. For example, IL-8 was one of the least cationic molecules studied (pI=9.0), but had greater efficacy than many of its more cationic counterparts.

#### 3.2.2. Solution-phase assay of native IL-8

Patterns of antimicrobial efficacy seen in diffusion assays of study kinocidins prompted further studies to examine microbicidal activity. Native (full-length) human IL-8 was selected as a prototype to characterize its microbicidal efficacy at pH 5.5 and 7.5 versus the pathogen panel. IL-8 was highly fungicidal for *C. albicans*, achieving a five-log reduction in surviving CFU with 2.5 nmol/ml (20  $\mu$ g/ml) peptide at pH 5.5 within 1 h (Fig. 4). IL-8 was also fungicidal for *C. albicans* at pH 7.5, with a 2-log reduction in surviving CFU over 1 h at a concentration of 2.5 nmol/ml. Interestingly, IL-8 did not exert microbicidal activity against *S. typhimurium* or *S. aureus* in this assay, suggesting that its efficacies versus these organisms in solid-phase assay were due to bacteriostatic effects.

Table 2  
Biochemical consensus patterns in human kinocidin primary structures

Signature	[C]	[X <sub>10-13</sub> ]	[G]	[X <sub>2-3</sub> ]	[C]	[X <sub>2</sub> ]	[P]								
Pattern	C	X <sub>3</sub>	X	X <sub>3</sub>	X <sub>0-2</sub>	X <sub>1-3</sub>	G	X	X <sub>2</sub>	C	Z	C	Z	D/N	P
Residue(s)	C	A/G/E/Q	(Z) <sub>3</sub>	K/R	G/B	K/R	B	Z	C	Z	D/N	P			
Frequency	97	100	>97	81	94	72	94	92	100	89	86	94			

Recurring patterns in amino acid residue are summarized relative to position in kinocidin  $\gamma$ -core motifs. For each component or position, the most common amino acid residue(s) are indicated, along with their percent frequency. Z represents the hydrophobic residues A, F, I, L, V, W, Y; B represents the charged or polar residues D, E, H, K, N, R, Q, S, T, C, P, or G correspond to cysteine, proline, or glycine, respectively; X indicates variable residues. Note a striking degree of conservation even within several variable positions (e.g., the hydrophobic triad [Z<sub>3</sub>] motif in the [X<sub>10-13</sub>] domain recurs with virtually 100% frequency across all kinocidins). Such high frequencies of conservation at multiple positions in the  $\gamma$ -core iterations, along with the presence of this motif in many classes of host defense polypeptides (e.g. kinocidins, antimicrobial peptides, peptide toxins, etc. [4,32]) imply a broader biological significance.

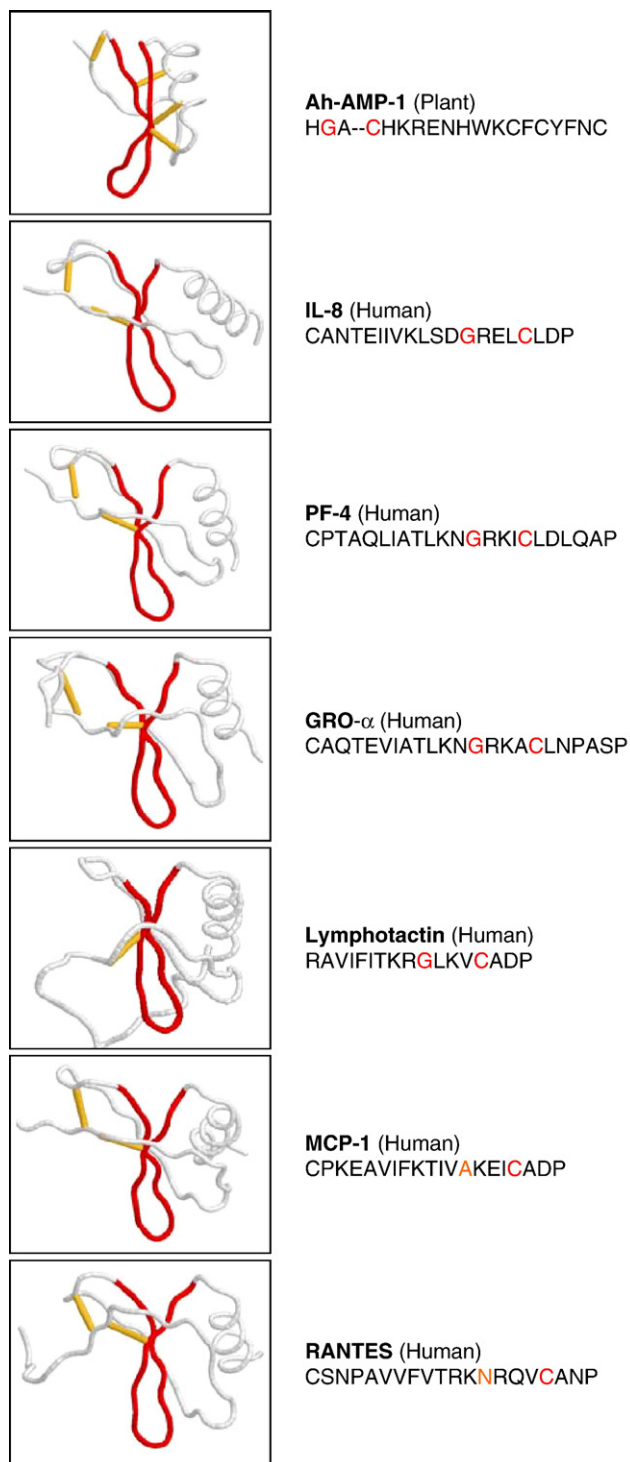


Fig. 2. Conservation of the  $\gamma$ -core domain ( $\gamma$ KC core) within diverse kinocidins. Recurring iterations of the  $\gamma$ KC core motif (red) are indicated with corresponding sequences (GX<sub>3</sub>C) denoted in red or gold text. A comparator antimicrobial peptide (Ah-AMP-1) is also shown to illustrate structural similarities between the  $\gamma$ KC motif and that present in antimicrobial peptides ( $\gamma$ AP). Proteins were visualized using protein explorer [18].

### 3.3. Structural determinants of IL-8 antimicrobial efficacy

Synthetic IL-8 $\gamma$  and IL-8 $\alpha$  peptides were used to probe for potential molecular correlates of antimicrobial activity.

#### 3.3.1. Solid-phase assay of IL-8 structural domains

IL-8 $\alpha$  displayed a spectrum of efficacy virtually indistinguishable from that of native IL-8 (Fig. 3). Importantly, the antimicrobial properties of native IL-8 were recapitulated by IL-8 $\alpha$  in the presence and absence of its corresponding  $\gamma$ -core motif (IL-8 $\gamma$ ), even though IL-8 $\gamma$  alone had no detectable antimicrobial efficacy at either pH 5.5 or 7.5. Thus, the antimicrobial efficacy of paired IL-8 $\alpha$  and IL-8 $\gamma$  was equivalent to their natural context in native IL-8 $\gamma$ .

#### 3.3.2. Solution-phase assay of IL-8 structural domains

In the solution-phase assay, as little as 0.125 nmol/ml (1.0  $\mu$ g/ml) of IL-8 $\alpha$  achieved a five-log reduction in surviving *C. albicans* at pH 5.5 in 1 h exposure (Fig. 4). By mass, the autonomous IL-8 $\alpha$  domain conferred a 10-fold greater activity than native IL-8 against this organism. The pH specific efficacy patterns of IL-8 $\alpha$  also mirrored those of full-length IL-8 (Fig. 4). Consistent with data in the solid-phase assay, IL-8 $\gamma$  had no measurable activity in the solution-phase assay, but did not impede efficacy of IL-8 $\alpha$ .

#### 3.3.3. Ex-vivo biomatrix assay

To assess putative physiological relevance of the observed *in vitro* antimicrobial activity of IL-8 and IL-8 $\alpha$ , the efficacy of IL-8 $\alpha$  was also tested in the *ex vivo* biomatrix assay. The *E. coli* strain ML-35 strain has been the organism of choice for this assay, as it is serum-resistant and thus serves as a highly relevant surrogate marker of infection. Importantly, IL-8 $\alpha$  exerted significant efficacy against *E. coli*, causing decreases of up to log 5 CFU/ml at 10  $\mu$ g/ml peptide (Fig. 5). Greatest efficacy was seen in whole blood and serum in co-incubation studies, with less activity in plasma fractions or after 2 h pre-incubation (Table 3).

### 3.4. Structure–activity relationships of IL-8 $\gamma$ and IL-8 $\alpha$ domains

To gain insights into their antimicrobial determinants, the structures of IL-8 $\gamma$  and IL-8 $\alpha$  were investigated using biophysical and computational methods:

#### 3.4.1. Spectrometry

CD spectrometry indicated that IL-8 $\gamma$  and IL-8 $\alpha$  recapitulated structures of corresponding regions in full-length IL-8 (Fig. 6). IL-8 $\gamma$  exhibited spectra consistent with a  $\beta$ -sheet structure, suggesting it spontaneously adopts a fold similar to that in native IL-8. Likewise, IL-8 $\alpha$  displayed classic double dichroic minima at 208 and 218 nm, hallmark of  $\alpha$ -helices, and concordant with the corresponding region in IL-8. These data suggest the forces responsible for secondary structures of these domains function independently from cysteine-stabilization or other constraints acting within the native molecule. Moreover, each structure was stable at pH 5.5 and pH 7.2 (Fig. 6).

#### 3.4.2. Computational modeling

To complement spectrometric studies, 3-D models of IL-8 $\gamma$  and IL-8 $\alpha$  were created using homology and energy-based

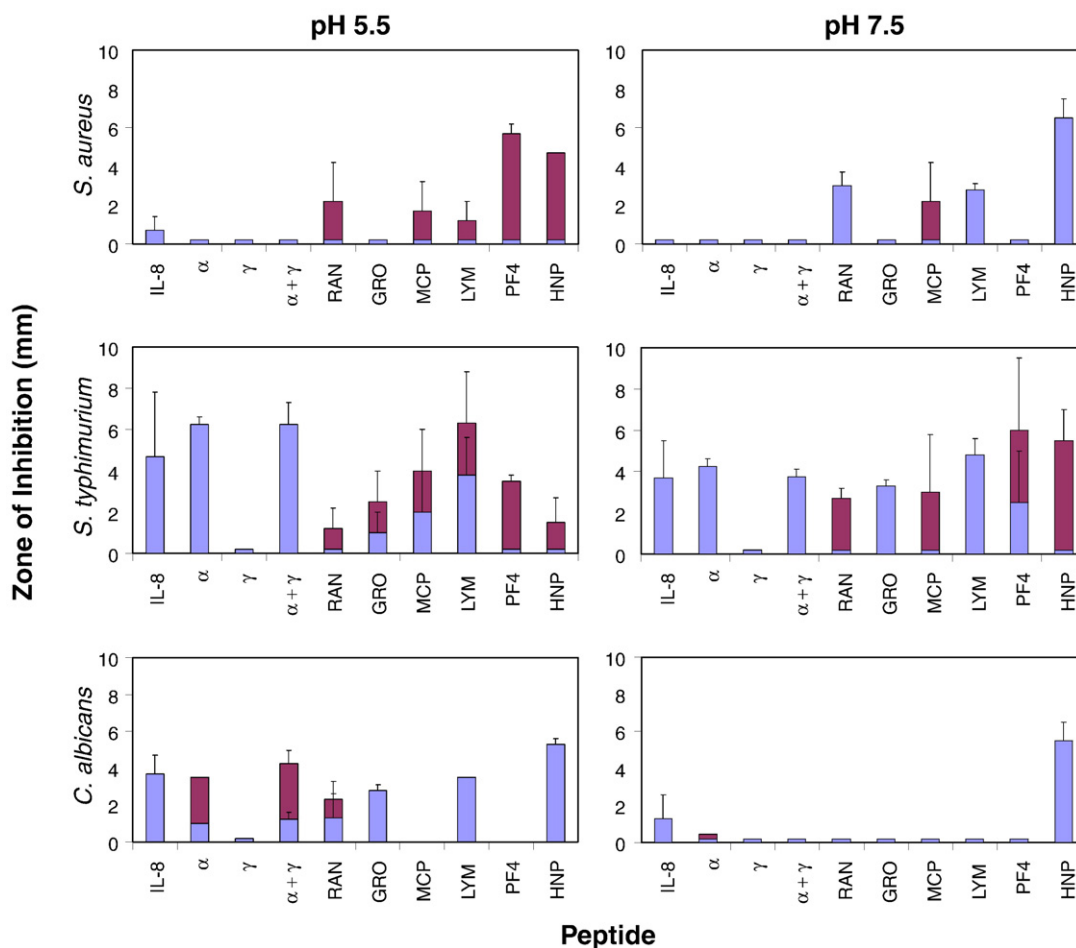


Fig. 3. Solid-phase antimicrobial activity of human kinocidins and IL-8 subdomains IL-8<sub>α</sub> and IL-8<sub>γ</sub>. Peptides (0.5 nmol) were introduced into wells in agarose plates buffered with MES (2.0 mM, pH 5.5) or PIPES (10.0 mM, pH 7.5). Antimicrobial activity was assessed as the zone of complete (blue) or partial (red) inhibition around the well. Abbreviations are: Native IL-8 (IL-8); IL-8<sub>α</sub> (α); IL-8<sub>γ</sub> (γ); IL-8<sub>α</sub>+IL-8<sub>γ</sub> (α+γ); RANTES, (RAN); GRO-α, (GRO); MCP-1, (MCP); lymphotactin, (LYM); platelet factor-4, (PF4); and HNP-1, (HNP). Histograms are means±SEM (minimum *n*=2).

methods. The template utilized for target peptide modeling was human IL-8 (PDB code, 1IL8). As expected, each peptide retained secondary structure corresponding to homologous domains within the native molecule (Fig. 7). The IL-8<sub>γ</sub> core motif displayed an anti-parallel β-sheet motif, while the preferential conformation for IL-8<sub>α</sub> was a highly stable α-helical motif comprised of four turns. These structure assignments are strongly supported by favorable empirical energy functions, equivalent to those of the IL-8 template.

#### 4. Discussion

Chemokines are essential regulators of cellular trafficking and immune signaling. However, until recently the possibility that chemokines might have direct roles as antimicrobial effector molecules had not been systematically investigated. The realization that mammalian platelets contain kinocidins [6,7] necessitated an expansion of the physiologic repertoire of activity for chemokines. These discoveries prompted investigation into whether other members of the structurally-conserved chemokine superfamily have direct antimicrobial effects.

Direct antimicrobial activity of kinocidins has been established in recent studies [7–11], as has the presence of γ-core motifs in disulfide-stabilized antimicrobial peptides and other host defense polypeptides [32]. However, the present studies are novel in that they identify specific γ-core signatures in kinocidins, further unifying structure and function in diverse host defense polypeptide classes. In addition, these studies provide the first evidence to our knowledge of direct antimicrobial activity of MCP-1, affirm our prior observations of the direct antimicrobial activities of native IL-8 [4,13,32], and reveal specific antimicrobial optima of these and other kinocidins. These investigations also provide new information regarding the direct microbicidal efficacy of native IL-8 and the IL-8<sub>α</sub> motif *in vitro* and in human blood biomatrices *ex vivo*.

The precise roles of specific amino acid residues comprising the γ-core motif of antimicrobial effector molecules is not yet known. Interestingly, several recent studies indicate that certain residues comprising γ-core motifs can be mutated with no significant change in antimicrobial efficacy [33–36]. For example, conversion from folded to linear form by cysteine deletion did not abrogate *in vitro* antimicrobial activity in derivatives of human β-defensin 3 [33,34], or in tachyplesins

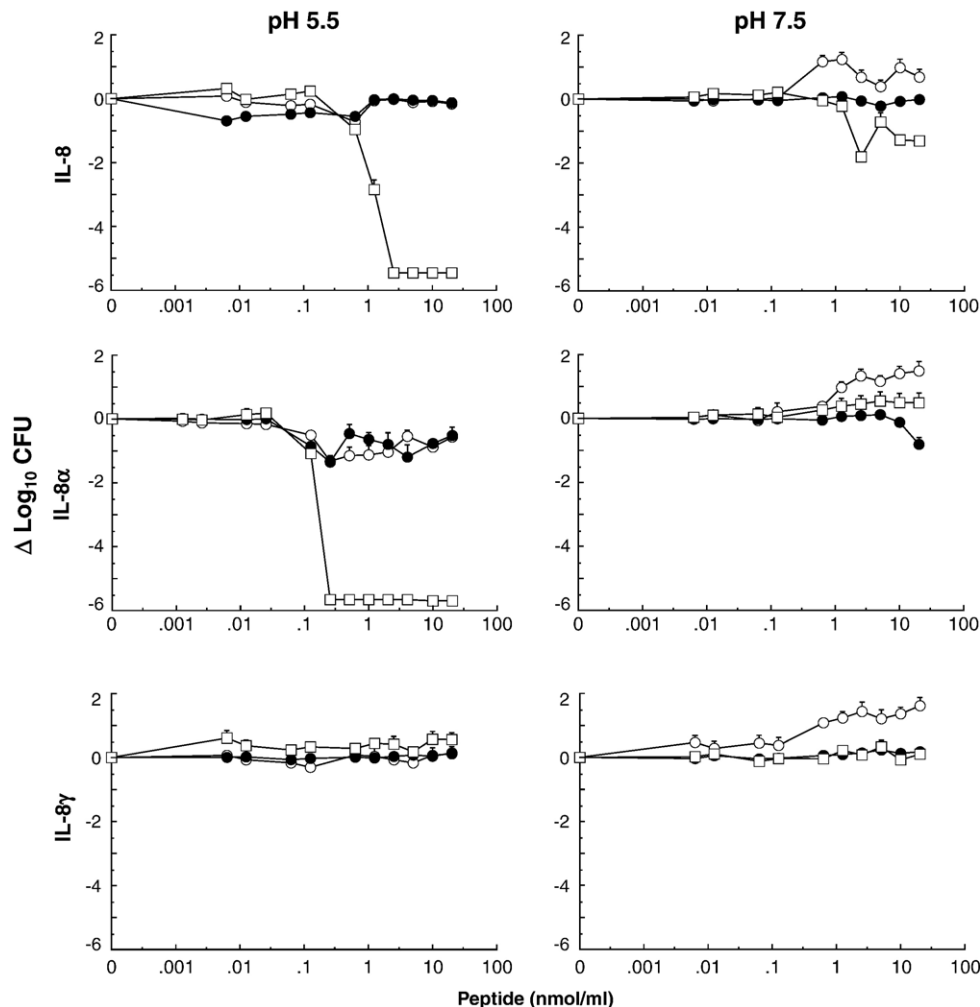


Fig. 4. Solution-phase microbicidal activity of native IL-8 and subdomains IL-8 $_{\alpha}$  and IL-8 $_{\gamma KC}$ . One million CFU of the indicated microorganism per milliliter were incubated with peptide (0.00125–20.0 nmol/ml) in either MES (2.0 mM, pH 5.5) or PIPES (10.0 mM, pH 7.5) for 1 h at 37 °C. Surviving CFU were enumerated and are described as change in the initial log<sub>10</sub> CFU. ○, *S. aureus* ATCC 27217; ●, *S. typhimurium* strain 5990 s; □, *C. albicans* ATCC 36082. Data are means±SD (minimum  $n=2$ ).

[36]. In contrast, other studies suggest key residues in the GXC element of the  $\gamma$ -core motif enable formation of a  $\beta$ -bulge associated with correct folding [37]. Whether similar structure–function correlates also hold true in kinocidins is not known. Nonetheless,  $\gamma$ -core motifs in IL-8 and perhaps other kinocidins may not confer direct antimicrobial activity, or may serve a scaffold-like role facilitating efficacy of its microbicidal helix [12,32]. For example, as disulfide-containing host defense proteins are generated through complex biosynthetic pathways,  $\gamma$ -core motifs may have primary roles in folding, trafficking, or deployment of kinocidins, rather than a direct antimicrobial function.

The fact that the  $\alpha$ -helical domain of IL-8 has autonomous microbicidal function implies that kinocidins are modular in configuration. Such kinocidins share a common topology comprised of a central  $\beta$ -sheet domain and  $\alpha$ -helix. Likewise, CS- $\alpha\beta$  family antimicrobial peptides. The strong antifungal activity of IL-8 observed in the current study correlates with its striking structural resemblance to classical antifungal CS- $\alpha\beta$  antimicrobial peptides of plants and insects, that also contain a

$\gamma$ -core and  $\alpha$ -helix [4] (Fig. 2); [4,32]. Alternatively, chemokine motifs are found in N-terminal domains of kinocidins. Such modular forms of kinocidins may facilitate proteolytic disassembly in contexts of infection, liberating complementary functional modules [12].

Investigation of the IL-8 $_{\alpha}$  domain revealed a highly ordered helix. As its helical conformation is highly stable at pH 5.5 and 7.5 (Fig. 6), pH-specific antimicrobial efficacy of IL-8 $_{\alpha}$  relies on parameters other than conformation. The current studies demonstrate that cationic charge and amphipathicity are segregated in 3-dimensions over the 19-residue IL-8 $_{\alpha}$  domain (Fig. 7). These findings concur with prior NMR studies [38] of the IL-8  $\alpha$ -helix region. Its estimated pI of 10 and net charge of +2 (at pH 7) indicate cationic propensity greater than that of corresponding domains in most other study kinocidins. Furthermore, its amphipathicity (6.70; Table 1) is also relatively high, as hydrophobic moments  $>3.0$  are considered significant in terms of hydrophobic and hydrophilic amino acid segregation. It is of particular interest that the IL-8 $_{\alpha}$  domain shares many physicochemical features with classical  $\alpha$ -helical

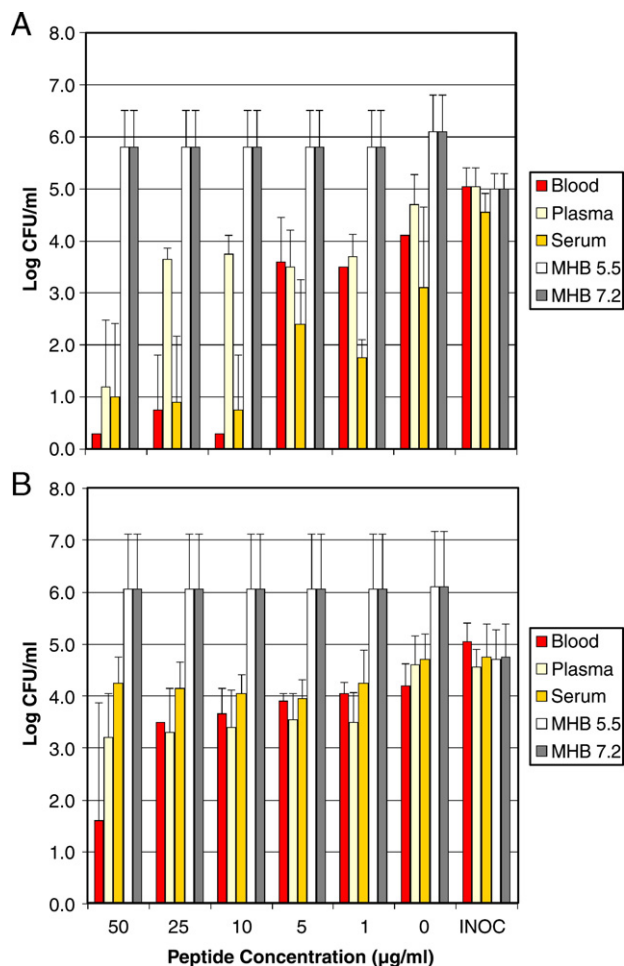


Fig. 5. Antimicrobial efficacy of IL-8 $\alpha$  in human blood and blood-derived matrices as compared with artificial media (MHB) at pH 5.5 and 7.2. (A) Co-incubation of IL-8 $\alpha$  and the organism simultaneously added to the test biomatrix or medium; (B) pre-incubation of IL-8 $\alpha$  in biomatrices or media for 2 h at 37 °C prior to introduction of the organism. The *E. coli* inocula (INOC) were  $10^5$  CFU/ml, and the threshold of sensitivity was considered 0.3 log<sub>10</sub> CFU/ml. Results are presented as mean  $\pm$  SD of a minimum of two independent experiments.

antimicrobial peptides derived from diverse precursors and sources such as the magainins [39,40] or LL-37 [41,42]. Many excellent studies have demonstrated that the cationic and amphipathic properties of these helical peptides are essential for microbicidal efficacy [41,43–46]. Future studies will address

Table 3  
Structural comparisons among representative human kinocidins

Class	Ligand ID	Name	PDB	RMSD	Z	Aln	Gap	%ID
CC	CCL2	MCP-1	1MCA	0.7	7.1	63	1	25
CXC	CXCL4	PF-4	1RHP	1.6	5.7	63	1	37
CXC	CXCL1	GRO- $\alpha$	1MGS	1.6	6.1	66	1	42
C	XCL1	Lymphotactin	1J8I	1.6	5.1	55	1	22
CC	CCL5	RANTES	1RTO	2.4	3.9	54	8	19

Prototypic kinocidins were aligned with human IL-8 (PDB: 1IL8) using combinatorial extension (Shindyalov and Bourne). Abbreviations: RMSD, root mean square deviation (calculated between  $\alpha$ -carbons); Z, z-score; Aln, number of residues aligned; Gap, gaps inserted for alignment; % ID, percent sequence identity with IL-8 over aligned region. Note that molecules are listed in ascending RMSD rank order.

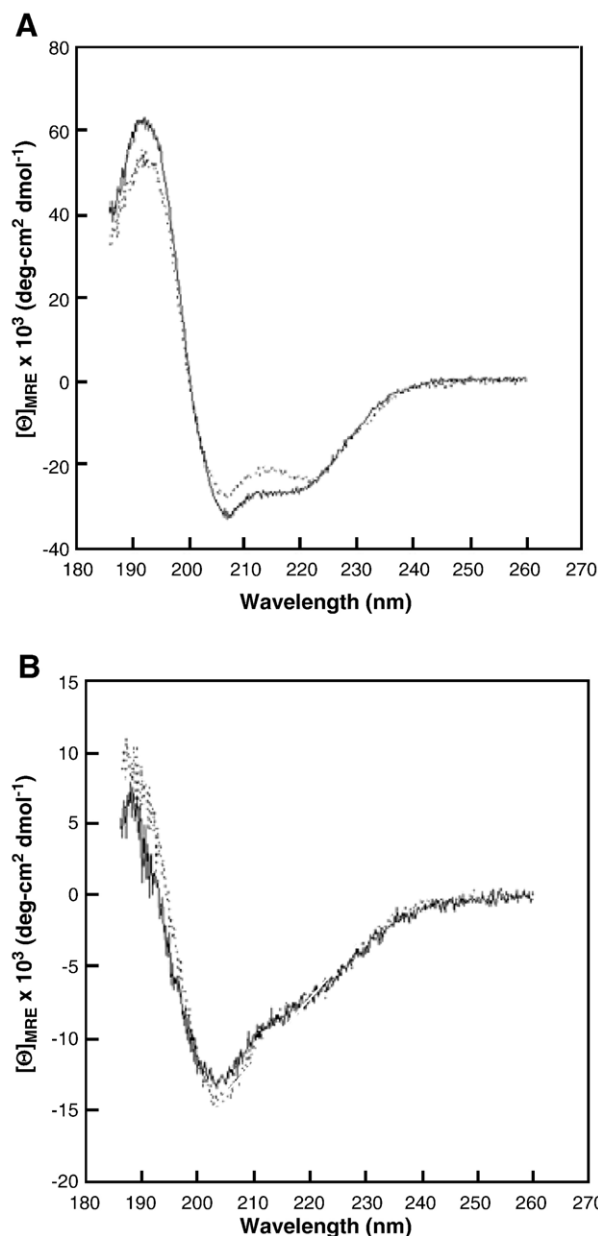


Fig. 6. Circular dichroism spectroscopy for IL-8 structural domains. The spectra were determined for the IL-8 $\alpha$  (A) and IL-8 $\gamma$  (B) peptides (0.1 mM) in sodium phosphate (10.0 mM, pH 5.5 [—]) or PIPES (10.0 mM, pH 7.5 [---]) buffer.

whether IL-8 $\alpha$  interacts with membranes in a manner similar to classical  $\alpha$ -helical antimicrobial peptides.

Guided by similarities to other kinocidins such as platelet microbicidal proteins [4,8], we previously identified direct and pH-related antimicrobial activity of full-length human IL-8 *in vitro* [4,8,12,13]. Meritorious prior studies did not detect antimicrobial activity of IL-8 or MCP-1 against bacteria [10,11], and their antifungal activity has not been shown previously. Thus, the present results provide new information, including demonstration of direct microbicidal efficacies of IL-8 and IL-8 $\alpha$ , with potent fungicidal activity versus *C. albicans*. The ability to detect IL-8 antimicrobial efficacy in the current studies may be due to a number of factors, including organism and/or strain differences, as well as buffer composition and pH.



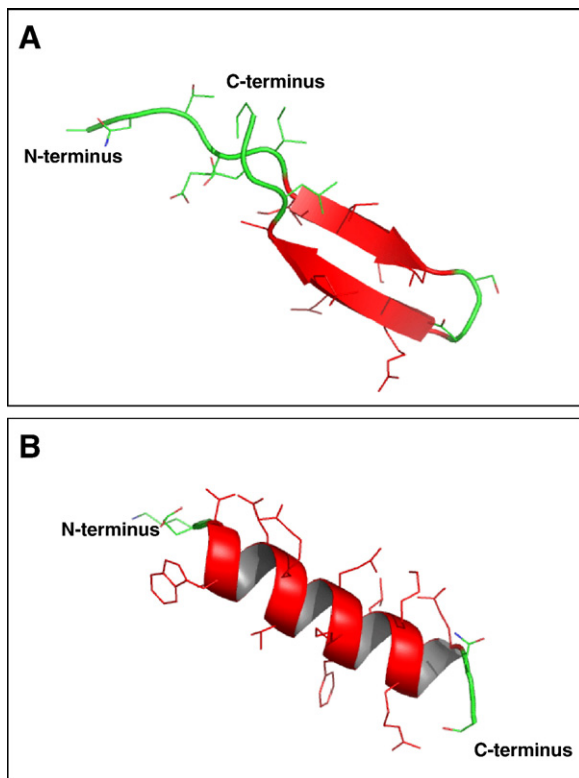


Fig. 7. Computational modeling of IL-8 structural domains. Three-dimensional models of IL-8 $\gamma_{KC}$  (A) and IL-8 $\alpha$  (B) peptides were created using homology and energy-based methods. Model peptide alpha-carbon backbones were visualized using PyMOL (version 0.97; 2004).

Prior studies using a radial diffusion assay measured activity against different organisms (*E. coli* or *Listeria monocytogenes*), and did not assess activity at pH 5.5 [10]. In the one prior study using a solution-phase assay, activity of IL-8 was evaluated against *E. coli* and *S. aureus* using a phosphate-based buffer system at pH 7.4 [11]. Results from these latter experiments corroborate the present finding that native IL-8 lacks activity against *S. typhimurium* or *S. aureus* in solution phase at pH 7.5.

One limitation to understanding the relevance of antimicrobial peptides is the need to determine their efficacy in biologically relevant settings. Importantly, the present data demonstrate previously unrecognized efficacy of the IL-8 $\alpha$  motif in human blood matrices. In this complex environment, IL-8 $\alpha$  was highly efficacious against *E. coli* at concentrations as low as 1–5  $\mu\text{g}/\text{ml}$ , with microbicidal activity at concentrations of 10  $\mu\text{g}/\text{ml}$  or more in blood. These discoveries are significant for several reasons. First, they substantiate the concept that autonomous kinocidin fragments exert microbicidal efficacy in relevant contexts. Second, IL-8 $\alpha$  has durable efficacy, since it exhibited microbicidal efficacy in serum fractions on co-incubation, and retained activity in blood matrices even after 2 h of pre-incubation before addition of the target pathogen. Prior studies with many antimicrobial peptides suggest substantial reductions in efficacy, inactivation in serum, or lack of efficacy in animal models [47,48]. Thus, the present data provide important

new insights toward understanding the direct antimicrobial roles of IL-8 or related kinocidins in relevant contexts *in vivo*.

Several lines of evidence support the concept that kinocidins exert direct antimicrobial activity in specific contexts in the host. For example, in normal human plasma, IL-8 is present at a very low baseline level in the range of pg/ml [49]. However, in acute contexts of infection, IL-8 levels can rise 1000-fold, reaching concentrations of 30–50 ng/ml [49]. In the current report, IL-8 $\alpha$  exerted substantial activity in blood matrices in the range of 50–500 ng/ml, a level consistent with that measured *in vivo*. Likewise, recent studies by Qiu et al. show that the chemokine CCL22/MDC intensifies to similar levels in lung granulomae [50]. Moreover, as they adhere to pathogens,  $\alpha$ -helical peptides derived from kinocidin-like holoproteins accumulate at sites of infection even after systemic administration [51]. Thus, measurements of their free concentration in media or sera almost certainly underestimate their local intensification [52]. Likewise, in sites of infection or inflammation (e.g. interstitial fluids, abscess exudates, serum, or mucosa), and in leukocyte phagolysosomes [53], pH can be significantly lower than that of plasma. The fact that many kinocidins, including IL-8 and IL-8 $\alpha$  have enhanced antimicrobial efficacy at pH 5.5 versus pH 7.5 is consistent with these concepts.

In summary, the novel findings define  $\gamma$ -core motifs in kinocidins, characterize structural and conditional correlates of kinocidin microbicidal activity, and demonstrate relevant microbicidal efficacy of IL-8 $\alpha$  in human blood matrices. This evidence supports the concept that kinocidins or their modules provide direct microbicidal efficacy in relevant physiological contexts [12], complementing their chemoattractant roles, thereby coordinating molecular and cellular host defenses. Together, these new insights support a reassessment of host defense functions traditionally ascribed to chemokines.

## Acknowledgements

This work was supported in-part by grants AI-39001, AI-48031 (MRY and NYY) and RR-14857 (MRY and AJW), from the National Institutes of Health (NIAID), and MCB-9817605 from the National Science Foundation (WHW). Some of these studies were performed at the Los Angeles Biomedical Research Institute at Harbor-UCLA Medical Center, Torrance, CA, and the Center for Health Sciences, UCLA.

## References

- [1] E. Hoffmann, O. Dittrich-Breiholz, H. Holtmann, M. Kracht, Multiple control of interleukin-8 gene expression, *J. Leukocyte Biol.* 72 (2002) 847–855.
- [2] A. Walz, P. Peveri, H. Aschauer, M. Baggiolini, Purification and amino acid sequencing of NAF, a novel neutrophil-activating factor produced by monocytes, *Biochem. Biophys. Res. Commun.* 149 (1987) 755–761.
- [3] T. Yoshimura, K. Matsushima, S. Tanaka, E.A. Robinson, E. Appella, J.J. Oppenheim, E.J. Leonard, Purification of a human monocyte-derived neutrophil chemotactic factor that has peptide sequence similarity to other host defense cytokines, *Proc. Natl. Acad. Sci. U. S. A.* 84 (1987) 9233–9237.

- [4] N.Y. Yount, M.R. Yeaman, Multidimensional signatures in antimicrobial peptides, *Proc. Natl. Acad. Sci. U. S. A.* 101 (2004) 7363–7368.
- [5] D. Yang, O. Chertov, S.N. Bykovskaia, Q. Chen, M.J. Buffo, J. Shogan, M. Anderson, J.M. Schroder, J.M. Wang, O.M. Howard, J.J. Oppenheim, Beta-defensins: linking innate and adaptive immunity through dendritic and T cell CCR6, *Science* 286 (1999) 525–528.
- [6] Y.Q. Tang, M.R. Yeaman, M.E. Selsted, Antimicrobial peptides from human platelets, *Infect. Immun.* 70 (2002) 6524–6533.
- [7] M.R. Yeaman, Y.Q. Tang, A.J. Shen, A.S. Bayer, M.E. Selsted, Purification and in vitro activities of rabbit platelet microbicidal proteins, *Infect. Immun.* 65 (1997) 1023–1031.
- [8] N.Y. Yount, K.D. Gank, Y.Q. Xiong, A.S. Bayer, T. Pender, W.H. Welch, M.R. Yeaman, Platelet microbicidal protein 1: structural themes of a multifunctional antimicrobial peptide, *Antimicrob. Agents Chemother.* 48 (2004) 4395–4404.
- [9] J. Krijgsveld, S.A. Zaai, J. Meeldijk, P.A. van Veelen, G. Fang, B. Poolman, E. Brandt, J.E. Ehlert, A.J. Kuijpers, G.H. Engbers, J. Feijen, J. Dankert, Thrombocidins, microbicidal proteins from human blood platelets, are C-terminal deletion products of CXC chemokines, *J. Biol. Chem.* 275 (2000) 20374–20381.
- [10] A.M. Cole, T. Ganz, A.M. Liese, M.D. Burdick, L. Liu, R.M. Strieter, Cutting edge: IFN-inducible ELR-CXC chemokines display defensin-like antimicrobial activity, *J. Immunol.* 167 (2001) 623–627.
- [11] D. Yang, Q. Chen, D.M. Hoover, P. Staley, K.D. Tucker, J. Lubkowski, J.J. Oppenheim, Many chemokines including CCL20/MIP-3 $\alpha$  display antimicrobial activity, *J. Leukocyte Biol.* 74 (2003) 448–455.
- [12] M.R. Yeaman, N. Yount, Code among chaos: immunorelativity and the AEGIS model of antimicrobial peptides, *ASM News* 71 (2005) 21–27.
- [13] M.R. Yeaman, Antimicrobial peptides: context drives strategy, 43rd Interscience Conference on Antimicrobial Agents and Chemotherapy (ICAAC), vol. 43, Chicago, IL, 2003.
- [14] A. Bjorstad, H. Fu, A. Karlsson, C. Dahlgren, J. Bylund, Interleukin-8-derived peptide has antibacterial activity, *Antimicrob. Agents Chemother.* 49 (2005) 3889–3895.
- [15] R.I. Lehrer, A. Barton, K.A. Daher, S.S. Harwig, T. Ganz, M.E. Selsted, Interaction of human defensins with *Escherichia coli*. Mechanism of bactericidal activity, *J. Clin. Invest.* 84 (1989) 553–561.
- [16] M.R. Yeaman, K.D. Gank, A.S. Bayer, E.P. Brass, Synthetic peptides that exert antimicrobial activities in whole blood and blood-derived matrices, *Antimicrob. Agents Chemother.* 46 (2002) 3883–3891.
- [17] Performance Standards for Antimicrobial Susceptibility Testing, Fourteenth Informational Supplement, NCCLS, Wayne, 2004.
- [18] E. Martz, Protein explorer: easy yet powerful macromolecular visualization, *Trends Biochem. Sci.* 27 (2002) 107–109.
- [19] D.G. Higgins, P.M. Sharp, CLUSTAL: a package for performing multiple sequence alignment on a microcomputer, *Gene* 73 (1988) 237–244.
- [20] I.N. Shindyalov, P.E. Bourne, Protein structure alignment by incremental combinatorial extension (CE) of the optimal path, *Protein Eng.* 11 (1998) 739–747.
- [21] D.C. Sheppard, M.R. Yeaman, W.H. Welch, Q.T. Phan, Y. Fu, A.S. Ibrahim, S.G. Filler, M. Zhang, A.J. Waring, J.E. Edwards Jr., Functional and structural diversity in the Als protein family of *Candida albicans*, *J. Biol. Chem.* 279 (2004) 30480–30489.
- [22] N. Sreerama, S.Y. Venyaminov, R.W. Woody, Estimation of the number of alpha-helical and beta-strand segments in proteins using circular dichroism spectroscopy, *Protein Sci.* 8 (1999) 370–380.
- [23] A. Lobley, L. Whitmore, B.A. Wallace, DICHROWEB: an interactive website for the analysis of protein secondary structure from circular dichroism spectra, *Bioinformatics* 18 (2002) 211–212.
- [24] W.K. Surewicz, H.H. Mantsch, New insight into protein secondary structure from resolution-enhanced infrared spectra, *Biochim. Biophys. Acta* 952 (1988) 115–130.
- [25] E. Goormaghtigh, V. Rausens, J.M. Ruyschaert, Attenuated total reflection infrared spectroscopy of proteins and lipids in biological membranes, *Biochim. Biophys. Acta* 1422 (1999) 105–185.
- [26] N. Guex, M.C. Peitsch, SWISS-MODEL and the Swiss-PdbViewer: an environment for comparative protein modeling, *Electrophoresis* 18 (1997) 2714–2723.
- [27] T. Schwede, J. Kopp, N. Guex, M.C. Peitsch, SWISS-MODEL: an automated protein homology-modeling server, *Nucleic Acids Res.* 31 (2003) 3381–3385.
- [28] X. Huang, W. Miller, A time-efficient, linear-space local similarity algorithm, *Adv. Appl. Math.* 12 (1991) 337–367.
- [29] A. Godzik, A. Kolinski, J. Skolnick, Topology fingerprint approach to the inverse protein folding problem, *J. Mol. Biol.* 227 (1992) 227–238.
- [30] L. Jaroszewski, L. Rychlewski, B. Zhang, A. Godzik, Fold prediction by a hierarchy of sequence, threading, and modeling methods, *Protein Sci.* 7 (1998) 1431–1440.
- [31] W.D. Cornell, P. Cieplak, C.I. Bayly, I.R. Gould, K.M. Merz, D.M. Ferguson, D.C. Spellmeyer, T. Fox, J.W. Caldwell, P.A. Kollman, A second generation force field for the simulation of proteins, nucleic acids, and organic molecules, *J. Am. Chem. Soc.* 117 (1995) 5179–5197.
- [32] N.Y. Yount, M.R. Yeaman, Structural congruence among membrane-active host defense polypeptides of diverse phylogeny, *Biochim. Biophys. Acta* 1758 (2006) 1373–1386.
- [33] Z. Wu, D.M. Hoover, D. Yang, C. Boulegue, F. Santamaria, J.J. Oppenheim, J. Lubkowski, W. Lu, Engineering disulfide bridges to dissect antimicrobial and chemotactic activities of human beta-defensin 3, *Proc. Natl. Acad. Sci. U. S. A.* 100 (2003) 8880–8885.
- [34] D.M. Hoover, Z. Wu, K. Tucker, W. Lu, J. Lubkowski, Antimicrobial characterization of human beta-defensin 3 derivatives, *Antimicrob. Agents Chemother.* 47 (2003) 2804–2809.
- [35] E. Kluver, S. Schulz-Maronde, S. Scheid, B. Meyer, W.G. Forssmann, K. Adermann, Structure–activity relation of human beta-defensin 3: influence of disulfide bonds and cysteine substitution on antimicrobial activity and cytotoxicity, *Biochemistry* 44 (2005) 9804–9816.
- [36] A. Ramamoorthy, S. Thennarasu, A. Tan, K. Gottipati, S. Sreekumar, D.L. Heyl, F.Y. An, C.E. Shelburne, Deletion of all cysteines in tachyplesin I abolishes hemolytic activity and retains antimicrobial activity and lipopolysaccharide selective binding, *Biochemistry* 45 (2006) 6529–6540.
- [37] C. Xie, A. Prah, B. Ericksen, Z. Wu, P. Zeng, X. Li, W.Y. Lu, J. Lubkowski, W. Lu, Reconstruction of the conserved beta-bulge in mammalian defensins using D-amino acids, *J. Biol. Chem.* 280 (2005) 32921–32929.
- [38] G.M. Clore, E. Appella, M. Yamada, K. Matsushima, A.M. Gronenborn, Three-dimensional structure of interleukin 8 in solution, *Biochemistry* 29 (1990) 1689–1696.
- [39] K. Matsuzaki, K. Sugishita, K. Miyajima, Interactions of an antimicrobial peptide, magainin 2, with lipopolysaccharide-containing liposomes as a model for outer membranes of gram-negative bacteria, *FEBS Lett.* 449 (1999) 221–224.
- [40] R.A. Cruciani, J.L. Barker, S.R. Durell, G. Raghunathan, H.R. Guy, M. Zasloff, E.F. Stanley, Magainin 2, a natural antibiotic from frog skin, forms ion channels in lipid bilayer membranes, *Eur. J. Pharm.* 226 (1992) 287–296.
- [41] U.H. Durr, U.S. Sudheendra, A. Ramamoorthy, LL-37, the only human member of the cathelicidin family of antimicrobial peptides, *Biochim. Biophys. Acta* 1758 (2006) 1408–1425.
- [42] V. Nizet, T. Ohtake, X. Lauth, J. Trowbridge, J. Rudisill, R.A. Dorschner, V. Pestonjams, J. Piraino, K. Huttner, R.L. Gallo, Innate antimicrobial peptide protects the skin from invasive bacterial infection, *Nature* 414 (2001) 454–457.
- [43] F. Porcelli, B.A. Buck-Koehntop, S. Thennarasu, A. Ramamoorthy, G. Veglia, Structures of the dimeric and monomeric variants of magainin antimicrobial peptides (MSI-78 and MSI-594) in micelles and bilayers, determined by NMR spectroscopy, *Biochemistry* 45 (2006) 5793–5799.
- [44] A. Mecke, D.K. Lee, A. Ramamoorthy, B.G. Orr, M.M. Banaszak Holl, Membrane thinning due to antimicrobial peptide binding: an atomic force microscopy study of MSI-78 in lipid bilayers, *Biophys. J.* 89 (2005) 4043–4050.
- [45] K.A. Henzler-Wildman, G.V. Martinez, M.F. Brown, A. Ramamoorthy, Perturbation of the hydrophobic core of lipid bilayers by the human antimicrobial peptide LL-37, *Biochemistry* 43 (2004) 8459–8469.
- [46] K.A. Henzler Wildman, D.K. Lee, A. Ramamoorthy, Mechanism of lipid bilayer disruption by the human antimicrobial peptide, LL-37, *Biochemistry* 42 (2003) 6545–6558.

- [47] R.I. Lehrer, A.K. Lichtenstein, T. Ganz, Defensins: antimicrobial and cytotoxic peptides of mammalian cells, *Annu. Rev. Immunol.* 11 (1993) 105–128.
- [48] A.V. Panyutich, P.S. Hiemstra, S. van Wetering, T. Ganz, Human neutrophil defensin and serpins form complexes and inactivate each other, *Am. J. Respir. Cell. Mol. Biol.* 12 (1995) 351–357.
- [49] A.S. Moller, A. Bjerre, B. Brusletto, G.B. Joo, P. Brandtzaeg, P. Kierulf, Chemokine patterns in meningococcal disease, *J. Infect. Dis.* 191 (2005) 768–775.
- [50] B. Qiu, K.A. Frait, F. Reich, E. Komuniecki, S.W. Chensue, Chemokine expression dynamics in mycobacterial (type-1) and schistosomal (type-2) antigen-elicited pulmonary granuloma formation, *Am. J. Pathol.* 158 (2001) 1503–1515.
- [51] P.H. Nibbering, M.M. Welling, A. Paulusma-Annema, C.P. Brouwer, A. Lupetti, E.K. Pauwels, 99mTc-Labeled UBI 29-41 peptide for monitoring the efficacy of antibacterial agents in mice infected with *Staphylococcus aureus*, *J. Nucl. Med.* 45 (2004) 321–326.
- [52] S. Mezzano, M.E. Burgos, L. Ardiles, F. Olavarria, M. Concha, I. Caorsi, E. Aranda, D. Mezzano, Glomerular localization of platelet factor 4 in streptococcal nephritis, *Nephron* 61 (1992) 58–63.
- [53] N.Y. Yount, M.R. Yeaman, Immunocontinuum: perspectives in antimicrobial peptide mechanisms of action and resistance, *Protein Pept. Lett.* 12 (2005) 49–67.
- [54] B. Bjellqvist, B. Basse, E. Olsen, J.E. Celis, Reference points for comparisons of two-dimensional maps of proteins from different human cell types defined in a pH scale where isoelectric points correlate with polypeptide compositions, *Electrophoresis* 15 (1994) 529–539.
- [55] R. Zidovetzki, B. Rost, D.L. Armstrong, I. Pecht, Transmembrane domains in the functions of Fc receptors, *Biophys. Chem.* 100 (2003) 555–575.